

# Measurement of $V_{ub}$

M. A. Selen

*Department of Physics, University of Illinois at Urbana-Champaign,  
Urbana, Illinois 61801-3080, USA*

The most recent experimental measurements of the weak mixing angle  $V_{ub}$  are summarized. Inclusive and exclusive analysis techniques are described, including a new exclusive analysis by the CLEO collaboration measuring the  $B \rightarrow \pi \ell \nu$  branching ratio. Future prospects are discussed.

## I. INTRODUCTION

The Standard Model of electroweak interactions is undeniably one of the most successful theories in particle physics, accommodating all observed phenomena to date. For all its glory, the theory has the undesirable feature that most of its parameters, although physically well motivated, must be determined empirically.

As an example, the way in which the weak interaction can mix quarks of different flavor is described by the Cabibbo-Kobayashi-Maskawa matrix [1,2]. The nine entries in this  $3 \times 3$  matrix contain information about the relative strengths and phases with which the  $(u, c, t)$  quarks couple to the  $(d, s, b)$  quarks, and their values must be measured experimentally. Our present knowledge of the magnitudes of these parameters are summarized below [3].

$$V = \begin{pmatrix} V_{ud} & V_{us} & V_{ub} \\ V_{cd} & V_{cs} & V_{cb} \\ V_{td} & V_{ts} & V_{tb} \end{pmatrix} = \begin{pmatrix} 0.9747 \rightarrow 0.9759 & 0.218 \rightarrow 0.224 & 0.002 \rightarrow 0.005 \\ 0.218 \rightarrow 0.224 & 0.9738 \rightarrow 0.9752 & 0.032 \rightarrow 0.048 \\ 0.004 \rightarrow 0.015 & 0.030 \rightarrow 0.048 & 0.9988 \rightarrow 0.9995 \end{pmatrix} \quad (1)$$

Note that the extreme diagonal elements,  $V_{ub}$  and  $V_{td}$ , are the least well determined.

In this paper the latest inclusive and exclusive measurements of the ratio  $|V_{ub}/V_{cb}|$  will be discussed. These were both made by the CLEO collaboration, using data accumulated at the Cornell Electron Storage Ring (CESR). In the CLEO-II detector, three concentric tracking devices provide charged-particle momentum resolution of  $\sigma_p/p = 0.005 + 0.0015p$  ( $p$  in GeV/c), and a 7800 crystal CsI calorimeter provides neutral shower energy resolution of  $\sigma_E/E = 0.019 - 0.001E + 0.0035/E^{0.75}$ . More detailed information is available elsewhere [4].

The data sample used in the inclusive analysis consists of  $924 \text{ pb}^{-1}$  accumulated with the CESR center of mass energy tuned to the  $\Upsilon(4S)$  resonance, and  $416 \text{ pb}^{-1}$  accumulated at energies below the  $B\bar{B}$  production threshold. The more recent exclusive analysis was done using approximately a factor of two more data.

## II. INCLUSIVE MEASUREMENTS

All determinations of  $V_{ub}$  to date have been made by studying charmless semileptonic decays of  $B$  mesons produced in  $e^+ - e^-$  collisions with center of mass energy at or near the  $\Upsilon(4S)$  resonance [5–9]. These are all measurements of the inclusive momentum-dependent rate of leptons,  $dN_\ell/dP_\ell$ , from  $B \rightarrow X_u \ell \nu$  decays [10].

Since the rate of  $b \rightarrow u \ell \nu$  is very small, the main experimental challenge in these analyses is the suppression of backgrounds. For inclusive  $b \rightarrow u \ell \nu$  analyses, the three main sources of unwanted leptons are  $b \rightarrow c \ell \nu$  decays, other  $B$  meson decays (for example  $B \rightarrow \psi X, \psi \rightarrow \ell^+ \ell^-$ ), and continuum (non  $B\bar{B}$ ) events. “Fake” leptons, for example  $\pi$ ’s that penetrate the detector iron and are misidentified as  $\mu$ ’s, must also be considered.

### A. $b \rightarrow c \ell \nu$ Suppression

The elimination of  $b \rightarrow c \ell \nu$  decays from the  $b \rightarrow u \ell \nu$  sample is achieved with a simple lepton momentum cut. As can be seen in Fig. 1(a), the kinematic endpoint momentum of leptons from  $B \rightarrow X_c \ell \nu$  is about 2.4 GeV/c [11]. Fig. 1(b) shows theoretical lepton spectra for several models of  $b \rightarrow u \ell \nu$  [12–14]. Although the models differ significantly in detail, they all share the basic kinematic feature that the lepton momentum endpoint extends to  $P_\ell \sim 2.6 \text{ GeV/c}$ .

The approach taken in all inclusive analyses has been to examine the yield of leptons only in the endpoint region between  $\sim 2.4$  GeV/c and 2.6 GeV/c [15]. This restriction eliminates most of the  $b \rightarrow cl\nu$  contamination, but only at the price of introducing a severe model-dependence in the procedure used to extract  $V_{ub}$  from the data. The reason for this is clear upon examination of Fig. 1(b). The models shown differ considerably, both in overall rate (plot area) and lepton momentum dependence (plot shape). The effect of these differences are discussed in a later section.

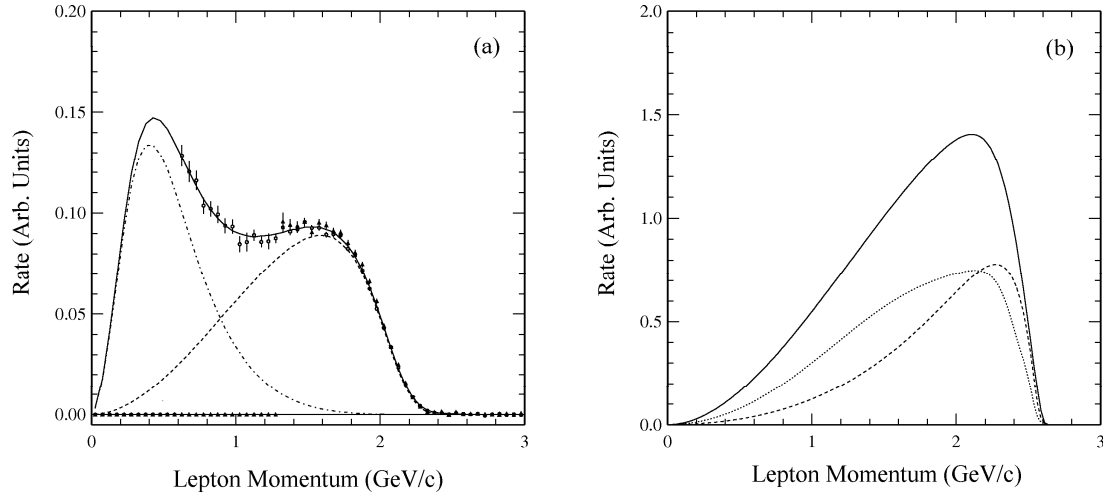


FIG. 1. (a) Inclusive lepton momentum spectrum showing the  $b \rightarrow cl\nu$  (dashed line) and  $b \rightarrow c \rightarrow yl\nu$  (dot-dashed line) components, as well as the total fit to CLEO data using the ACCMM model (solid line). (b) The predicted  $b \rightarrow ul\nu$  lepton momentum spectra for the ACCMM (solid line), ISGW (dotted line) and WSB (dashed line) models.

## B. Continuum Suppression

Leptons from non- $B\bar{B}$  continuum events, for example  $e^+e^- \rightarrow c\bar{c}$ ,  $c \rightarrow sl\nu$ , are not kinematically excluded from the inclusive  $b \rightarrow ul\nu$  signal region between 2.4 and 2.6 GeV/c. This is a large source of background, and is dealt with in two steps. First, a set of continuum suppression requirements are used to eliminate most of these events. Second, the remaining background is removed by subtracting the luminosity scaled lepton spectrum obtained by analyzing “signal free” data accumulated at center of mass energies below the  $B\bar{B}$  production threshold.

The most powerful continuum suppression requirements are topological in nature, designed to select the typically spherical  $B\bar{B}$  events while rejecting the more “jetty” continuum background. The shape variable used by CLEO is the Fox-Wolfram parameter  $R_2 = H_2/H_0$  [16]. The missing momentum of an event,  $p_{miss}$ , provides additional discrimination against continuum processes. This quantity should be large for  $b \rightarrow ul\nu$  events where the neutrino carries off appreciable momentum. The requirements that  $R_2 < 0.2$ , that  $p_{miss} > 1$  GeV/c, and that the lepton and missing momentum point into opposite hemispheres are used. The net effect of these cuts is to reduce the continuum background by a factor of 70 while maintaining 38% efficiency for the  $b \rightarrow ul\nu$  signal.

The statistical uncertainty introduced by the continuum subtraction is a function of the size of the continuum data sample. The normal operating mode of CESR/CLEO-II is to accumulate data on the  $\Upsilon(4S)$  resonance two-thirds of the time, and just below  $B\bar{B}$  threshold the remaining one-third. The resulting continuum data sample is large enough that the error introduced by the subtraction are much smaller than the statistical error on the signal yield.

## C. Other Backgrounds

After continuum suppression and subtraction, the events remaining in the lepton momentum endpoint region are either true  $b \rightarrow ul\nu$  signal or non-continuum background. This background is due to leptons from

$b \rightarrow c \rightarrow X\ell\nu$ , from  $B \rightarrow \psi$  and  $B \rightarrow \psi'$  decays, and from fake leptons. The fraction of events in the lepton spectrum signal region due to these sources is less than 10%, is well understood from studying the data, and is carefully accounted for when calculating the final  $b \rightarrow u\ell\nu$  yield.

#### D. Signal Extraction and Model Dependence

Fig. 2(a) shows lepton spectra from  $\Upsilon(4S)$  and continuum data. The solid line is a fit to the continuum lepton distribution. Fig. 2(b) shows the result of luminosity scaling and subtracting this fitted line from the  $\Upsilon(4S)$  data, as well as the predicted contribution from  $b \rightarrow c\ell\nu$  decays. A significant excess of events is seen, indicating the presence of charmless B decays.

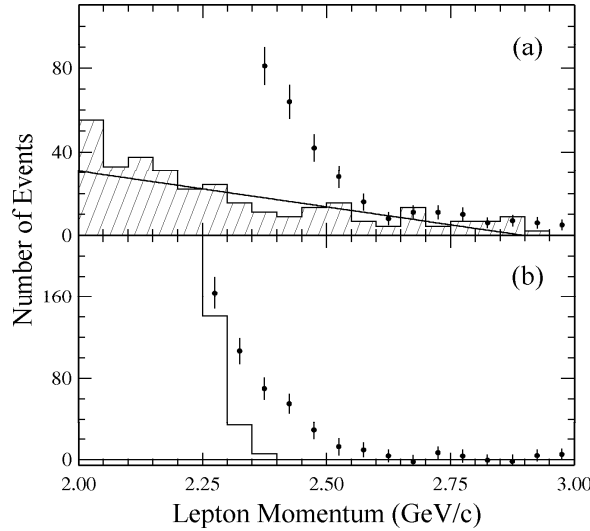


FIG. 2. CLEO-II inclusive lepton momentum distributions. Shown in (a) are lepton spectra from  $\Upsilon(4S)$  (filled circles) and continuum (hatched histogram) data, as well as a fit to the continuum lepton distribution (solid line). The filled circles in (b) show the result of subtracting the fitted and scaled continuum distribution from the  $\Upsilon(4S)$  data. The solid histogram shows the predicted contribution from  $b \rightarrow c\ell\nu$  decays.

Extracting  $|V_{ub}/V_{cb}|$  from the endpoint data involves several model dependent factors:

$$\left| \frac{V_{ub}}{V_{cb}} \right| = \frac{\Delta B_{ub}(p)}{d(p)B_{cb}} \quad (2)$$

In this expression  $B_{cb}$  is the  $b \rightarrow c\ell\nu$  branching ratio and  $\Delta B_{ub}(p)$  is the partial branching ratio observed in the endpoint signal region [17]:

$$\Delta B_{ub}(p) = \frac{N_{ub}(p)/\epsilon(p)}{2N_{B\bar{B}}} \quad (3)$$

where  $N_{ub}(p)$  is the number of  $b \rightarrow u\ell\nu$  events in the signal region,  $\epsilon(p)$  is the detection efficiency for these events, and  $2N_{B\bar{B}}$  is the number of  $B$  mesons produced.  $\Delta B_{ub}(p)$  is somewhat model dependent since the detection efficiency  $\epsilon$  depends weakly on the shape of the lepton momentum spectrum.

The term  $d(p)$  is the product of several strongly model-dependent factors:

$$d(p) = f_u(p) \frac{\gamma_u}{\gamma_c} \quad (4)$$

where  $f_u(p)$  is the fraction of the total  $b \rightarrow u\ell\nu$  spectrum in the endpoint signal region (model dependence on spectrum shape), and  $\gamma_u$  relates the semileptonic width and  $V_{ub}$  via  $\Gamma_{b \rightarrow u\ell\nu} = \gamma_u |V_{ub}|^2$  [18], (model dependence on spectrum area).

Table I shows the factors  $d(p)$  and  $\epsilon(p)$  as well the final extracted CLEO values of  $\Delta B_{ub}(p)$  and  $|V_{ub}/V_{cb}|$  for various models. The model-dependence of  $|V_{ub}/V_{cb}|$  is larger than the experimental uncertainty, and at present is the biggest factor limiting the accuracy of this measurement.

TABLE I. CLEO-II results for  $d(p)$ ,  $\epsilon(p)$ ,  $\Delta B_{ub}(p)$  and  $|V_{ub}/V_{cb}|$ . The values listed for  $d(p)$  and  $\epsilon(p)$  were calculated for the momentum range  $2.4 < p_\ell(\text{GeV}/c) < 2.6$ , and are shown to illustrate the effect of model dependence. The values of  $\Delta B_{ub}(p)$  and  $|V_{ub}/V_{cb}|$  represent the extended signal region  $2.3 < p_\ell(\text{GeV}/c) < 2.6$ .

Model	$d(p)$	$\epsilon(p)$	$10^6 \times \Delta B_{ub}(p)$	$ V_{ub}/V_{cb} $
ACCMM [12]	0.12	$0.16 \pm 0.01$	$154 \pm 22 \pm 20$	$0.076 \pm 0.008$
ISGW [13]	0.05	$0.21 \pm 0.02$	$121 \pm 17 \pm 15$	$0.101 \pm 0.010$
WSB [14]	0.11	$0.20 \pm 0.02$	$122 \pm 17 \pm 16$	$0.073 \pm 0.007$
KS [19]	0.19	$0.22 \pm 0.02$	$115 \pm 16 \pm 15$	$0.056 \pm 0.006$

### III. EXCLUSIVE MEASUREMENTS

The CLEO collaboration has recently observed the exclusive charmless semileptonic decay mode  $B \rightarrow \pi \ell \nu$ . Measurement of this and other exclusive channels will provide a new avenue for determining  $|V_{ub}/V_{cb}|$  and studying the  $b \rightarrow u \ell \nu$  form factors, and should be a powerful tool for testing the various available models.

This section will provide some details of the CLEO  $B \rightarrow h \ell \nu$  analysis, where  $h$  is  $\pi^\pm$ ,  $\pi^0$ ,  $\rho^\pm$ ,  $\rho^0$  or  $\omega$ . Table II lists the theoretical predictions for the partial widths of  $B \rightarrow \pi \ell \nu$  and  $B \rightarrow \rho \ell \nu$ , and their ratio. Note again that the predicted widths show a strong model-dependence.

TABLE II. Predictions for the exclusive partial widths  $\Gamma(B^0 \rightarrow \pi^- \ell \nu)$  and  $\Gamma(B^0 \rightarrow \rho^- \ell \nu)$ .

Model	$\Gamma(B^0 \rightarrow \pi^- \ell \nu) [10^{12}  V_{ub} ^2 \text{ sec}^{-1}]$	$\Gamma(B^0 \rightarrow \rho^- \ell \nu) [10^{12}  V_{ub} ^2 \text{ sec}^{-1}]$	$\Gamma(B^0 \rightarrow \rho^- \ell \nu) / \Gamma(B^0 \rightarrow \pi^- \ell \nu)$
ISGW [13]	2.1	8.3	4.0
WSB [14]	6.3 – 10.0	18.7 – 42.5	3.0 – 4.3
KS [19]	7.25	33.0	4.6
ISGW II [20]	9.6	14.2	1.5
FGM [21]	$3.1 \pm 0.6$	$5.7 \pm 1.2$	$1.8 \pm 0.5$

#### A. Neutrino Reconstruction

The difficulty with exclusive reconstruction of semileptonic decays is the lack of knowledge of the undetected neutrino's 4-momentum. Using the large solid-angle coverage of the CLEO-II detector [22] to measure the *total* momentum and energy of the *rest* of the event, CLEO is able to infer  $(E_\nu, \vec{p}_\nu)$  of the neutrino from the missing momentum and energy  $(E_{\text{miss}}, \vec{p}_{\text{miss}})$  of the event as a whole:

$$E_\nu \sim E_{\text{miss}} = 2E_{\text{beam}} - E_{\text{meas}}^{\text{tot}} \quad \text{and} \quad \vec{p}_\nu \sim \vec{p}_{\text{miss}} = -\vec{p}_{\text{meas}}^{\text{tot}} \quad (5)$$

where  $E_{\text{meas}}^{\text{tot}}$  ( $\vec{p}_{\text{meas}}^{\text{tot}}$ ) is the total measured energy (momentum) of all tracks and showers in the event. Analysis of Monte Carlo generated  $B \rightarrow \pi \ell \nu$  events yields resolutions of 110 MeV and 260 MeV for  $|\vec{p}_\nu|$  and  $E_\nu$  respectively.

This method assumes the neutrino from  $b \rightarrow u \ell \nu$  is the only undetected particle, making it crucial to reject events containing additional unseen particles (neutrinos and/or  $K_L$ 's). This is accomplished by demanding that candidate events have only one identified lepton, have zero net charge, and that the reconstructed mass of the neutrino ( $m_\nu^2 = M_\nu^2 - P_\nu^2$ ) be consistent with zero [23].

Additional constraints are placed on the final state hadrons. Candidate  $\pi^0$ 's must have a  $2\gamma$  invariant mass within  $2\sigma$  (about 12 MeV) of the nominal  $\pi^0$  mass, and  $2\pi$  ( $3\pi$ ) combinations must have invariant mass within 90 MeV (30 MeV) of the  $\rho$  ( $\omega$ ) mass. Identified leptons are required to have a momentum greater than 1.5 GeV/c (2.0 GeV/c) in the  $\pi \ell \nu$  ( $\rho/\omega \ell \nu$ ) modes.

For events passing the above neutrino, meson, and lepton selection requirements, the reconstructed “beam constrained”  $B$  mass  $m_B \equiv \sqrt{E_{beam}^2 - |\vec{p}_h + \vec{p}_\ell + \vec{p}_\nu|^2}$  and energy difference  $\Delta E \equiv E_{beam} - (E_h + E_\ell + |\vec{p}_\nu|)$  are calculated. Real  $B \rightarrow h\ell\nu$  events should have  $\Delta E$  close to zero and  $m_B$  close to the  $B$  meson rest mass. Monte Carlo studies are used to determine the optimum location of the signal region in the  $\Delta E - m_B$  plane, finding  $-250 < \Delta E(\text{MeV}) < 150$  and  $5.265 < m_B(\text{GeV}/c^2) < 5.2875$ .

As in the inclusive analysis, event shape variables [16] are used to suppress continuum backgrounds, and a continuum subtraction is done. The contribution from fake leptons is studied using data, and is also subtracted. The remaining background is predominantly due to  $b \rightarrow c\ell\nu$  decays containing an additional  $\nu$  or  $K_L$ , and to cross-feed from other  $b \rightarrow u\ell\nu$  modes.

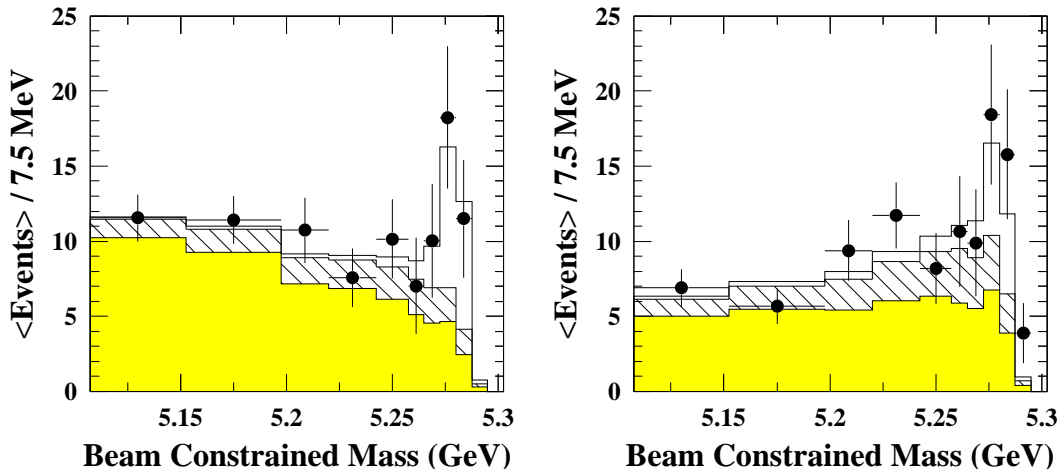


FIG. 3. Beam constrained mass distributions for combined  $\pi\ell\nu$  (left) and  $\rho\ell\nu$  (right) modes. The points are continuum and fake subtracted data, the histograms show the contribution from signal (hollow),  $b \rightarrow c\ell\nu$  (shaded), and  $b \rightarrow u\ell\nu$  cross-feed (hatched).

### B. Signal Extraction and Model Dependence

After subtracting the contributions from continuum and fake leptons and selecting events in the  $\Delta E$  signal region, the beam-constrained mass ( $m_B$ ) distributions of the five signal modes are simultaneously fitted. The shapes of the  $b \rightarrow c\ell\nu$  and cross-feed background contributions are obtained from Monte Carlo. The normalization of the  $b \rightarrow c\ell\nu$  background for each mode are free parameters in the fit. The isospin relations  $\frac{1}{2}\Gamma(B^0 \rightarrow \pi^-\ell^+\nu) = \Gamma(B^+ \rightarrow \pi^0\ell^+\nu)$  and  $\frac{1}{2}\Gamma(B^0 \rightarrow \rho^-\ell^+\nu) = \Gamma(B^+ \rightarrow \rho^0\ell^+\nu) \approx \Gamma(B^+ \rightarrow \omega\ell^+\nu)$  constrain the relative neutral and charged meson rates. The total signal and cross-feed background for all five modes is in this way parameterized by two numbers  $N_\pi$  and  $N_\rho$ , the total yield of  $\pi$  events and  $\rho$  events respectively.

The beam-constrained mass distributions for  $B \rightarrow \pi\ell\nu$  and  $B \rightarrow \rho\ell\nu$  are shown in Fig. 3. The results of the fit for the case of  $B \rightarrow \pi\ell\nu$  are summarized in Table III, where the signal yield, efficiency,  $b \rightarrow c\ell\nu$  background, and  $b \rightarrow u\ell\nu$  cross-feed probabilities are shown for both the ISGW and WSB models. Note that although the yields are very similar for both models, the efficiencies differ significantly. The contribution from higher mass and non-resonant  $b \rightarrow u\ell\nu$  modes, denoted “other  $u\ell\nu$ ”, is fixed by inclusive lepton endpoint spectrum measurements.

Many checks have been performed to verify that the observed signal is real, including fitting the energy difference ( $\Delta E$ ) distribution rather than the beam-constrained mass, examining the lepton momentum spectrum and the distribution of angles between the pion and the lepton in the  $W$  rest-frame. More details of these studies, as well as a discussion of systematic errors, can be found elsewhere [24].

TABLE III. Backgrounds, efficiencies and fit results for the  $B \rightarrow \pi \ell \nu$  analysis.

	$\pi^- \ell \nu$		$\pi^0 \ell \nu$	
	ISGW	WSB	ISGW	WSB
Raw Data		30		15
Continuum Bkg.		$2.3 \pm 0.8$		$1.0 \pm 0.5$
Fake Lepton Bkg.		$1.2 \pm 0.3$		$0.7 \pm 0.2$
other $u\ell\nu$ Bkg.		0.6		0.2
Efficiency	2.9%	2.1%	1.9%	1.4%
Signal Yield	$15.6 \pm 5.3$	$16.3 \pm 5.3$	$5.0 \pm 1.7$	$5.3 \pm 1.7$
$b \rightarrow c$ Bkg.	$9.8 \pm 1.1$	$9.8 \pm 1.1$	$1.8 \pm 0.5$	$1.7 \pm 0.5$
$\rho/\omega$ Bkg.	$3.8 \pm 1.7$	$3.4 \pm 1.4$	$1.8 \pm 0.8$	$1.6 \pm 0.7$

Correcting the yield for efficiency results in a preliminary measurement of the  $B \rightarrow \pi \ell \nu$  branching ratio:  $\mathcal{B}(B^0 \rightarrow \pi^- \ell \nu) = (1.19 \pm 0.41) \times 10^{-4}$  using ISGW and  $(1.70 \pm 0.55) \times 10^{-4}$  using WSB. The errors shown are statistical only.

For the vector meson modes the fit results are used to calculate an upper limit rather than a branching ratio since the non-resonant contribution is uncertain. Using the conservative assumption that there is no non-resonant  $b \rightarrow u\ell\nu$  background present in the  $B \rightarrow \rho\ell\nu$  signal region, the 90% confidence level upper limits for  $\mathcal{B}(B^0 \rightarrow \rho^- \ell \nu)$  is found using the ISGW (WSB) model to be  $< 3.1 \times 10^{-4}$  ( $< 4.6 \times 10^{-4}$ ), consistent with the upper limits previously published by CLEO [25].

One of the more interesting quantities that can be extracted from the data is an upper limit on the *ratio* of branching ratios  $\mathcal{B}(B^0 \rightarrow \rho^- \ell \nu)/\mathcal{B}(B^0 \rightarrow \pi^- \ell \nu) < 3.4$  at the 90% confidence level for both WSB and ISGW models. This can be directly compared to the ratio of partial widths found in Table II.

#### IV. CONCLUSIONS AND FUTURE PROSPECTS

At present, the limiting uncertainty in  $|V_{ub}/V_{cb}|$  is theoretical. The statistical error of the inclusive measurements is about 10%, and the variation between models is at least twice as large. Even within a single model, variation of parameters within reasonable limits can yield significant changes [26]. CLEO is in the process of repeating its inclusive analysis with over than a factor of two more data, which will further decrease the statistical error of the endpoint analysis.

Experiments can do more, however, to provide guidance to the theoretical community. With sufficient statistics, measuring the  $q^2$  distribution of leptons in the inclusive endpoint region should provide useful feedback. The model dependence can in principle be reduced, or at the very least explored, by examining data in different regions of the  $q^2 - p_\ell$  plane.

Semileptonic  $\Lambda_b$  decays may provide another avenue to study  $V_{ub}$ . A measurement of the form factors in  $\Lambda_c \rightarrow \Lambda \ell \nu$  can be related to  $\Lambda_b \rightarrow p \ell \nu$  using SU(3) and HQET, and used to extract  $|V_{ub}/V_{cb}|$  [27]. Several authors have discussed ways of relating the differential spectra for  $b \rightarrow u\ell\nu$  and  $b \rightarrow s\gamma$  to reduce the uncertainty in the endpoint region due to hadronization [28–31].

The statistical significance of exclusive measurements is still poor, but will improve with experimental running. It is unlikely that exclusive analyses will ever surpass inclusive measurements in terms of raw statistical accuracy, however they will certainly provide a very powerful tool for testing various theoretical models. The experimental limit on the ratio  $\mathcal{B}(B^0 \rightarrow \rho^- \ell \nu)/\mathcal{B}(B^0 \rightarrow \pi^- \ell \nu) < 3.4$  at 90% confidence level is already slightly challenging for some. Other measurements such as lepton momentum spectra,  $q^2$  distribution, and vector meson polarization will provide further theoretical tests [32]. Exclusive measurements at low  $q^2$  may also prove valuable [33]. It has recently been shown that measurements of  $B \rightarrow \rho\ell\nu$  and  $B \rightarrow K^* \ell \bar{\ell}$  can be used to extract  $V_{ub}$  using SU(3) and HQET [34].

The theoretical problem of determining the form factors needed to calculate  $b \rightarrow u\ell\nu$  is also being approached with lattice gauge calculations, and several groups are making progress [35–38].

In conclusion, good theoretical and experimental progress is being made in the quest to determine  $|V_{ub}/V_{cb}|$ , and the next few years should yield significant advances in both.

I would like to thank Jeff Nelson, Ron Poling, Lawrence Gibbons and Ed Thorndike for information about the latest CLEO analyses. I would also like to thank John Sloan and Aida El-Khadra for insight regarding

lattice calculations, and finally I would like to acknowledge Tom Browder and Klaus Honscheid whose review paper “B Mesons” provided valuable information and references.

I gratefully acknowledge the support of the Department of Energy and the A. P. Sloan Foundation.

- [1] N. Cabibbo, Phys. Rev. Lett. **10**, 531 (1963).
- [2] M. Kobayashi and K. Maskawa, Prog. Theor. Phys. **49**, 282 (1972).
- [3] Particle Data Group Phys. Rev. D **50**, 1 (1994).
- [4] Y. Kubota *et al.* Nucl. Instrum. & Methods **A320**, 66 (1992).
- [5] The CLEO collaboration, Phys. Rev. Lett. **64**, 16 (1990).
- [6] The ARGUS collaboration, Phys. Lett. B **234**, 409 (1990).
- [7] The ARGUS collaboration, Phys. Lett. B **255**, 297 (1991).
- [8] The CLEO collaboration, Phys. Rev. Lett. **71**, 4111 (1993).
- [9] Ph.D. thesis of J. K. Nelson, University of Minnesota (1994).
- [10] Both electrons and muons are used in these analyses.
- [11] This assumes that the  $B$  meson is produced in the reaction  $e^+e^- \rightarrow \Upsilon(4S) \rightarrow B\bar{B}$ .
- [12] G. Altarelli *et al.*, Nucl. Phys. B **208**, 365 (1982).
- [13] N. Isgur *et al.*, Phys. Rev. D **39**, 799 (1989).
- [14] M. Wirbel *et al.*, Z. Phys. C **29**, 637 (1985).
- [15] The 1993 CLEO analysis described here used an extended signal region:  $2.3 < P_\ell(\text{GeV}/c) < 2.6$ .
- [16] G. Fox and S. Wolfram, Phys. Rev. Lett. **41**, 1581 (1978).
- [17]  $(p)$  indicates that the quantity is a function of the endpoint momentum interval chosen.
- [18]  $\gamma_c$  is similarly defined via  $\Gamma_{b \rightarrow c\ell\nu} = \gamma_c |V_{cb}|^2$ .
- [19] J. Körner and G. Schuler, Z. Phys. C **38**, 511 (1988).
- [20] N. Isgur and D. Scora, CEBAF preprint CEBAF-TH-94-14.
- [21] R. Faustov *et al.*, hep-ph/9505321.
- [22] The CLEO-II tracking and calorimeter systems cover respectively 95% and 98% of  $4\pi$ .
- [23] The requirement  $M_\nu^2/2E_\nu < 350$  MeV is used since the  $M_\nu^2$  resolution varies approximately as  $2E_\nu^2\sigma_{E_\nu}$ .
- [24] L. Gibbons, talk at *30th Rencontres de Moriond* (1995): hep-ex/9508012.
- [25] The CLEO collaboration, Phys. Rev. Lett. **70**, 2681 (1993).
- [26] D. Hwang *et al.*, hep-ph/9502346.
- [27] A. Datta, hep-ph/9504429.
- [28] A. Falk *et al.*, Phys. Rev. D **49**, 4553 (1994).
- [29] M. Neubert, Phys. Rev. D **49**, 4623 (1994).
- [30] I. Bigi *et al.*, Int. J. Mod. Phys. **A 9**, 2467 (1994).
- [31] G. Korchemsky and G. Sterman, Phys. Lett. B **340**, 96 (1994).
- [32] R. Faustov *et al.*, hep-ph/9508262.
- [33] Akhoury *et al.* Phys. Rev. D **50**, 358 (1994).
- [34] A. Sanda and A. Yamada hep-ph/9507283.
- [35] G. Martinelli, Talk presented at *6'th International Symposium of Heavy Flavor Physics*, Pisa (1995).
- [36] The UKQCD Collaboration, hep-ph/9506398.
- [37] The APE Collaboration, hep-ph/9411011.
- [38] The LANL Collaboration, hep-ph/9501016.